

Determination of optimum load resistances of MQ-series gas sensor circuit for specific gas concentrations

TAIWO, Ajiboye Aye, FEMI, Opadiji Jayeola Femi Jayeola, RUTH, Ajayi Adebimpe and OLUSOGO, Popoola Joshua

Available from Sheffield Hallam University Research Archive (SHURA) at:

<https://shura.shu.ac.uk/34042/>

This document is the author deposited version. You are advised to consult the publisher's version if you wish to cite from it.

Published version

TAIWO, Ajiboye Aye, FEMI, Opadiji Jayeola Femi Jayeola, RUTH, Ajayi Adebimpe and OLUSOGO, Popoola Joshua (2022). Determination of optimum load resistances of MQ-series gas sensor circuit for specific gas concentrations. TELKOMNIKA (Telecommunication Computing Electronics and Control), 20 (1), 158-165.

Copyright and re-use policy

See <http://shura.shu.ac.uk/information.html>

Determination of optimum load resistances of MQ-series gas sensor circuit for specific gas concentrations

Ajiboye Aye Taiwo, Opadiji Jayeola Femi, Ajayi Adebimpe Ruth, Popoola Joshua Olusogo

Department of Computer Engineering, Faculty of Engineering and Technology, University of Ilorin, Ilorin, Nigeria

Article Info

Article history:

Received Jul 14, 2021

Revised Dec 18, 2021

Accepted Dec 29, 2021

Keywords:

Liquefied petroleum gas

MQ-6 gas sensor

Sensor circuit sensitivity

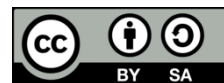
Sensor power dissipation

Sensor resistance

ABSTRACT

MQ-series gas sensors are frequently used in gas concentration sensing owing to their high sensitivity and relatively cheap cost. Reportedly, both the sensor's circuit sensitivity (S) and power dissipation (P_S) are functions of sensor circuit load resistance (R_L). However, there is no well-established standard method for determining R_L value that can simultaneously yield maximum sensor circuit sensitivity (S_M) and acceptable P_S for a given value of gas concentration. To obtain optimum R_L , the dependence of S and P_S on R_L for a given gas concentration was thoroughly investigated. The model equations for determining S, P_S and R_L at $S_M (R_{L,MAX})$ were derived and MQ-6 gas sensor's response to its associated gases was used for demonstrating the proposed method. Variations of both S and P_S with respect to R_L were investigated when each of the associated gases has concentration of 1000 ppm. The sensor circuit optimal R_L must satisfy the dual conditions of (i) $S=S_M$ and (ii) $P_S < \text{set threshold}$. Results obtained from the analysis revealed that the values of $R_{L,MAX}$ were 20, 24, 64, 120, and 152 k Ω for liquefied petroleum gas (LPG), CH₄, H₂, alcohol and CO respectively, corresponding to sensor powers of 0.3125, 0.2589, 0.0977, 0.0521, and 0.0411 mW.

This is an open access article under the [CC BY-SA](https://creativecommons.org/licenses/by-sa/4.0/) license.



Corresponding Author:

Ajiboye Aye Taiwo

Department of Computer Engineering, Faculty of Engineering and Technology, University of Ilorin

P.M.B. 1515, Ilorin, Nigeria

Email: ajiboye.at@unilorin.edu.ng

1. INTRODUCTION

MQ-series gas sensors are frequently employed in gas concentration sensing due to their high sensitivity and low cost compared to other alternatives [1]-[3]. This class of gas sensors consists of micro aluminium oxide (AL₂O₃) ceramic tube, a sensitive layer of tin dioxide (SnO₂), and nickel-chromium alloys that generate the necessary heat required for the desired sensor operation. The sensor is interfaced with the external circuits and components via 6 pins, out of which two are used each for signal, electrodes, and heating coils, respectively [4]-[6]. The SnO₂ semiconductor is the portion of the sensor that senses the gas [4], [5], [7], [8] and it has a variable resistance with gas concentration and the type; and it also possesses high resistance in clean air [9]. The sensor resistance varies with the gas concentration when they are placed in the vicinity of the gas to be sensed [8], [10], [11]. The magnitude of the sensor circuit output signal is a function of both the concentration and type of the gas [7], [9], [12] and the nature of metal oxide used for the sensor sensing area [2], [13], [14]. The heating and the sensing section of the sensor can be powered by a separate or same voltage source (s). This is to generate the required heat needed to maintain the sensor in the active state and the conversion of the sensed gas concentration to an appropriate voltage level across the load resistor in the sensor circuit [6], [10], [13], [15]. Due to the resistive nature of the sensor's sensing element, the sensed

gas concentration is normally converted to the voltage across the load resistor in the sensor circuit [6], [9], [10], [12].

The required sensor circuit parameters for the calibration and analysis of Metal Oxide (MOX) semiconductor gas sensors are: sensor activation voltage (V_{CC}), sensor circuit output voltage (V_{RL}), sensor resistance in the base gas at calibration concentration in clean air (R_0) [16], the sensor resistance (R_S) and load resistance (R_L) [4], [17]. In practice, the value of R_0 is usually determined experimentally [4], because it is only the range that is normally given in the sensor datasheet; and more so it is practically impossible to have gas sensors with the same value of R_0 [8], [11], [18]. Once the value of R_0 is determined, the sensor resistances at different gas concentrations can then be obtained from the sensor sensitivity curve in the sensor datasheet for various types of gases under given temperature and relative humidity (RH) [2].

Haija *et al.* [19], studied MQ-2 gas sensor was used to monitor air quality by adopting the 20 k Ω load resistance as given in the sensor datasheet. Rumantri *et al.* [4], presented an air quality monitoring system was developed consisting of an MQ-7 gas sensor and two others. But a load resistance of 1 K Ω was adopted in the study which is quite not within the range (5 k Ω - 47 k Ω) given in the datasheet with no justification given. The air quality monitoring system developed in [20] used MQ-2 gas sensor and a variable load resistance value (0-5 k Ω) to allow for sensitivity adjustment [21]. A combination of MQ-2, MQ-3, MQ-6, MQ-135, with a load resistance of 10 k Ω connected to each was used in [5] to develop a real-time olfaction monitoring system; however, the choice of using a load resistance of 10 k Ω for all the sensors was not given. The 20 k Ω load resistance recommended in the MQ-2 gas sensor datasheet was adopted in [22] for developing an air pollution monitoring system using a single MQ-2 gas sensor for both CO and smoke detection. The clean air sensor resistance for the MQ-5 gas sensor was determined in [1] by arbitrarily selecting 20 k Ω for the load resistance. In a death-defying gas intelligent sensor system [6], MQ-2 and MQ-7 were used for sensing flammable gases and carbon monoxide respectively but the load resistance value of 1 k Ω which is outside the range (5 k Ω - 47 k Ω) recommended in the sensor datasheet was used for both sensors. In the microcontroller-based liquefied petroleum gas (LPG) leakage monitoring and control systems proposed by [23]-[30], the leakage gas was sensed in these systems using MQ-2 [23], [27], MQ-6 [24], [25], [28], [29], MQ-5 [26], and MQ-4 [30] gas sensors. The load resistance value was arbitrarily selected for these systems. Maximum sensitivity and tolerable sensor power dissipation are the major factors required for the selection of load resistance at the alarm point [13], [31]. The load resistance should always be selected in such a way as to improve the sensor performance because when it is too low it results to low sensitivity and when it is high it gives less accuracy [22].

It was established in [3] that S and P_S both depend on R_L . However, there is no well-established existing standard method of determining R_L value that can simultaneously yield S_M and tolerable P_S for a given value of gas concentration. Also, the method employed in [3] assumed sensor circuit output voltage was linearly related to the gas concentration. Therefore, for the method to be effective, it must be applied to the linear portion of the relationship which will require additional efforts like physical inspection and/or linearity test on the plot to locate the portion. In this study, the non-linear relationship between the sensor circuit output voltage and gas concentration has no effect as the sensitivity can be determined for any given value of gas concentration. Therefore, the major contribution of this study is the development of a structured method of optimum load resistance determination for MQ-series gas sensors for any given gas concentration. This was achieved by investigating the dependence of both the sensor circuit sensitivity and power dissipation on the load resistance for a given gas type and concentration. Furthermore, the study will provide a standard method of load resistance determination for MQ-series gas sensor circuit designers.

Applying the sensor model equations proposed by [3], the equations for S , $R_{L,MAX}$ and P_S at a given gas concentration were derived. To demonstrate the proposed method, the response of MQ-6 gas sensor to its associated gases was considered. The MQ-6 gas sensor parameters were substituted into the S , P_S , and $R_{L,MAX}$ equations for the various gases. The curves of S and P_S were each plotted against R_L for a given value of R_0 and concentration. The plotted curves were used to study the trend of the observed variations. The value of $R_{L,MAX}$ and the corresponding value of P_S was determined for each of the gases. The R_L value that resulted in highest S and $P_S < \text{set threshold}$ is the optimum for the sensor circuit for a given gas and concentration value. Since the value of R_L that resulted in highest S and also satisfied the P_S condition for all the MQ-6 gas sensor associated gases is $R_{L,MAX}$, the optimum R_L for the MQ-6 gas sensor circuit will be $R_{L,MAX}$. The variation of $R_{L,MAX}$ with concentration and the effects of substituting $R_{L,MAX}$ for R_L on sensor circuit output voltage for MQ-6 gas sensor associated gases were also investigated.

2. METHODOLOGY

This section is devoted to development of the required model equations. The equations derived for S , P_S , and $R_{L,MAX}$ is presented in this section. Also, the application of the developed equations in the graphical

determination of the optimum load resistance, $R_{L,MAX}$ was demonstrated using MQ-6 gas sensor response to its associated gases. The detail analysis of the resulting graphs are presented in section 3.

2.1. Development of system model equations

The expression for sensor resistance in terms of gas concentration (x) and R_O is as shown in (1) [3].

$$R_S = 10^{(m \log_{10} x + \log_{10} c + \log_{10} R_O)} \quad (1)$$

$$m = \frac{\log_{10}(y_2) - \log_{10}(y_1)}{\log_{10}(x_2) - \log_{10}(x_1)} \quad (2)$$

Where (x_1, y_1) and (x_2, y_2) are the coordinates of any two different points on the straight line associated with a given gas on the sensor sensitivity characteristics curve.

$$c = 10^{(q)} \quad (3)$$

Where q is the point of intersection of the sensor sensitivity characteristics curve associated with a given gas with the $\frac{R_S}{R_O}$ -axis.

Also, the sensor circuit output voltage is given by (4) [3].

$$V_{RL} = \frac{R_L V_{CC}}{(R_S + R_L)} \quad (4)$$

Substituting (1) in (4) yielded (5).

$$V_{RL} = \frac{R_L V_{CC}}{(10^{(m \log_{10} x + \log_{10} c + \log_{10} R_O)} + R_L)} \quad (5)$$

As revealed in (5), V_{RL} is a function of x , R_O and R_L because V_{CC} , m , and c are constant for a given sensor circuit and gas type. It should be noted that the range of R_O and R_L for a particular MQ-series gas sensor is always specified in the sensor datasheet. Since R_L is the only parameter that can be varied by the circuit designer [3], its effect on the sensor circuit sensitivity and sensor power dissipation for a given value of x and R_O was investigated for its optimum selection. To select R_L , the highest sensor circuit sensitivity and tolerable sensor power dissipation conditions must be met [13].

The model equation for S was derived by differentiating (5) with respect to x and is expressed in (6).

$$S = \frac{-m V_{CC} R_L 10^{(m \log_{10} x + \log_{10} c + \log_{10} R_O)}}{x (10^{(m \log_{10} x + \log_{10} c + \log_{10} R_O)} + R_L)^2} \quad (6)$$

The relationship between P_S and sensor resistance, R_S is expressed in (7) [3].

$$P_S = \frac{V_{CC}^2 R_S}{(R_S + R_L)^2} \quad (7)$$

The expression for $R_{L,MAX}$ for a given value of x and R_O was obtained by finding the derivative of S in (6) with respect to R_L and then solve for R_L . The resulting model equation is as expressed in (8).

$$R_{L,MAX} = 10^{(m \log_{10} x + \log_{10} c + \log_{10} R_O)} \quad (8)$$

In (8) validates the proposition in (1). Using (6) and (7), the plots of S versus R_L and P_S versus R_L can be obtained and used to study the trend of variation between S and R_L ; and also P_S and R_L . This would allow graphical determination of the optimum value of R_L for a given value of R_O and x . Also, from (8), the plot of $R_{L,max}$ versus x can be generated for a given value of R_O . The value of R_O can be determined by using an empirical or graphical approach, the latter was applied in this study using the range of R_O given in the sensor datasheet. It should be noted that the maximum value of power dissipated by the sensor must not be greater than the permissible value [31].

2.2. Demonstration of the proposed method

To investigate the effects of variation of R_L on S and P_s , MQ-6 gas sensor was used and all the gases that can be sensed by this sensor were considered. The first step in the plot of S and P_s versus R_L is to determine the value of the following parameters: V_{CC} , x , m , c and R_O and then substitute them into (6) and (7). In this study $V_{CC} = 5\text{ V}$ and $x = 1000\text{ ppm}$ were adopted for all the gases while m and c were determined using (2) and (3) for each of the gases following the procedure explained in sub-section 2.1. To determine R_O , the graph of S versus R_L was plotted (using LPG being the base gas for MQ-6 gas sensor), for $10\text{ k}\Omega \leq R_L \leq 47\text{ k}\Omega$, $10\text{ k}\Omega \leq R_O \leq 60\text{ k}\Omega$ and $x = 1000\text{ ppm}$ as shown in Figure 1. The value of $R_{L,MAX}$ corresponding to R_O can be obtained from Figure 1.

Using (6) and (7), the plots of S versus R_L and P_s versus R_L for all MQ-6 gas sensor associated gases for $10\text{ k}\Omega \leq R_L \leq 180\text{ k}\Omega$ were plotted and are as shown in Figures 2 and 3 respectively. These plots were used to study the trend of variation of the sensor circuit sensitivity and sensor power dissipation with respect to load resistance. The value of $R_{L,MAX}$ when the sensor is under the influence of each of the gases were determined from Figure 2 and investigation of their compliance with the sensor power dissipation condition was carried out using Figure 3.

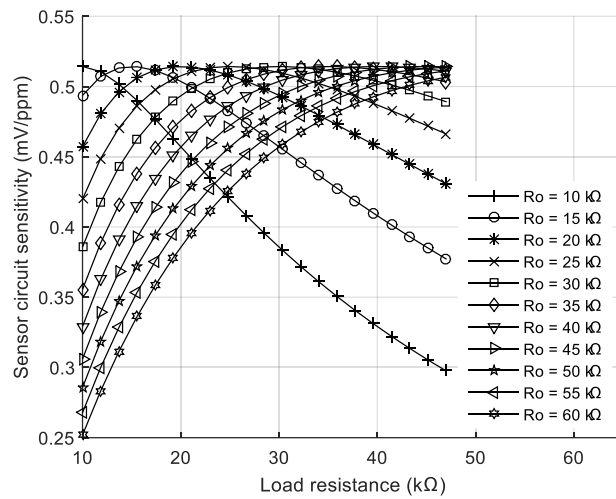


Figure 1. Plots of S versus R_L for $x = 1000\text{ ppm}$ at various R_O

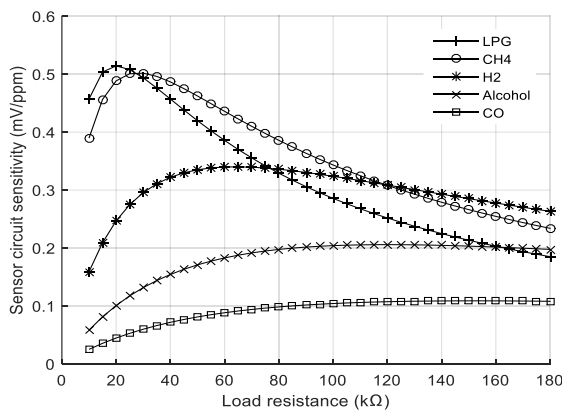


Figure 2. Plots of S versus R_L for $R_O = 20\text{ k}\Omega$ for all MQ-6 associated gases

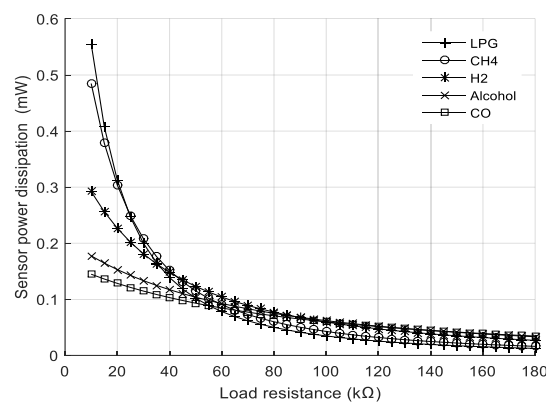


Figure 3. Plots of P_s versus R_L for $R_O = 20\text{ k}\Omega$ for all MQ-6 associated gases

Using (8), the plots of $R_{L,MAX}$ against x were carried out as shown in Figure 4 to study the variation of $R_{L,MAX}$ with x for each of the MQ-6 associated gases. Furthermore, by using (5), the graph of V_{RL} was also plotted against x for each of the gases as shown in Figure 5. In Figure 5, there are two plots on the same

graph, the solid line with markers (LPG-1, CH₄-1, H₂-1, Alcohol-1 and CO-1) is for the situation when $R_L = 20 \text{ k}\Omega$ for all the gases and the dash-dash line with markers (LPG-2, CH₄-2, H₂-2, Alcohol-2 and CO-2) is for when $R_L = R_{L,MAX}$. From this Figure, the effect of substituting $R_{L,MAX}$ for R_L on the sensor circuit output voltage can be quantified.

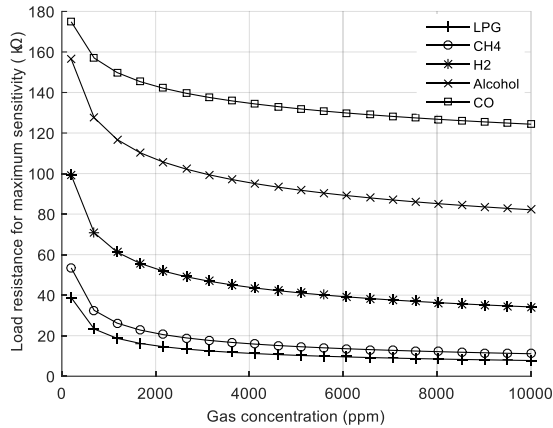


Figure 4. Plots of $R_{L,MAX}$ versus x for $R_O = 20 \text{ k}\Omega$ for all MQ-6 associated gases

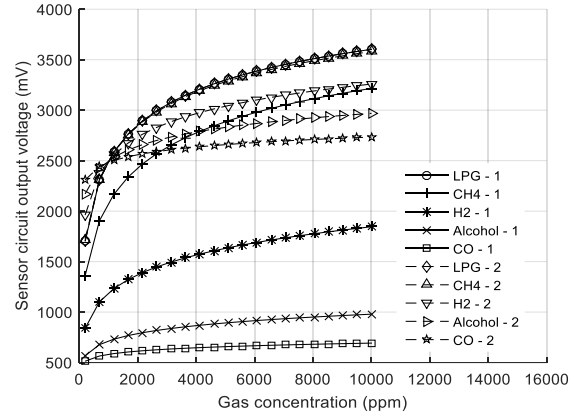


Figure 5. Plots of V_{RL} versus x for all MQ-6 gas sensor associated gases for $R_L = 20 \text{ k}\Omega$ (solid line) and $R_L = R_{L,MAX}$ (dash-dash line)

3. RESULTS AND DISCUSSIONS

The summary of the results obtained from Figure 1 is presented in Table 1. It can be seen from Table 1, that $R_O = R_{L,MAX}$ is consistent for $10 \text{ k}\Omega \leq R_L \leq 60 \text{ k}\Omega$ and $10 \text{ k}\Omega \leq R_O \leq 60 \text{ k}\Omega$ and the maximum sensitivity (S_M) remains constant at 0.5143 mV/ppm . In practice, $10 \text{ k}\Omega \leq R_L \leq 47 \text{ k}\Omega$ [32], but as can be seen from Table 1 to obtain S_M for any value of R_L the range of R_L and R_O must be same, therefore that of R_O ($10 \text{ k}\Omega \leq R_O \leq 60 \text{ k}\Omega$) was used in this study. It has been established by [32] that $R_S = R_O$ when MQ-6 gas sensor is in the vicinity of the base gas (LPG) at concentration of 1000 ppm and also from (1) and (8) that $R_S = R_{L,MAX}$, therefore, it can be inferred that $R_O = R_{L,MAX}$ for this sensor which supports the results presented in Table 1. Since the value of R_L used for the calibration of MQ-6 gas sensor at 1000 ppm of LPG in the datasheet is $20 \text{ k}\Omega$ [32], it was assumed that $R_{L,MAX} = 20 \text{ k}\Omega$ for this sensor which make $R_O = 20 \text{ k}\Omega$. This value is very close to what was obtained in [3] ($23 \text{ k}\Omega$).

Table 1. Summary of the relationship among R_O , $R_{L,MAX}$ and S_M

R_O (kΩ)	$R_{L,MAX}$ (kΩ)	S_M (mv/ppm)
10	10	0.5143
15	15	0.5143
20	20	0.5143
25	25	0.5143
30	30	0.5143
35	35	0.5143
40	40	0.5143
45	45	0.5143
50	50	0.5143
55	55	0.5143
60	60	0.5143

From Figure 2, it can be observed that the value of S increases from the initial value (S_i), when $R_L = 10 \text{ k}\Omega$, to the maximum value at $R_L = R_{L,MAX}$ for the various gases, after which it decreases to the final value (S_f) which corresponds to minimum value when $R_L = 180 \text{ k}\Omega$. The condition for R_L in the datasheet is $10 \text{ k}\Omega \leq R_L \leq 47 \text{ k}\Omega$, implying that if this range is used, the circuit will only attain its maximum sensitivity under the influence of LPG or CH₄. Therefore, the upper bound for R_L was extended to $180 \text{ k}\Omega$ to enable the circuit attain S_M for other three gases. As can be seen from Figure 2, the values of $R_{L,MAX}$ for LPG, CH₄, H₂,

Alcohol and CO are 20, 24, 64, 120 and 152 k Ω , respectively corresponding to S_M values of 0.5143, 0.5017, 0.3402, 0.2059 and 0.1089 mV/ppm. Apart from determining $R_{L,MAX}$ from Figure 2, once R_O value is determined from Figure 1, the value of $R_{L,MAX}$ for any of the gases at a given concentration can be determined from the sensor sensitivity curves normally given in the sensor datasheet since it has been revealed in this study that $R_S = R_{L,MAX}$ at a given concentration for all gases. It should be noted that for the sensor circuit to satisfy the maximum sensitivity requirements the condition $R_L = R_{L,MAX}$ must be fulfilled for the concerned gas.

It can be observed from Figure 3 that, the initial power dissipation value ($P_{S,i}$) obtained at $R_L = 10$ k Ω is the highest value for the sensor when it is under the influence of each of the gases. As R_L increases, P_S decreases from $P_{S,i}$ to the final value ($P_{S,f}$) when $R_L = 180$ k Ω . The values of sensor power dissipation when $R_L = R_{L,MAX}$ ($P_{S,RL,MAX}$) for LPG, CH₄, H₂, Alcohol and CO were obtained from Figure 3 as 0.3125, 0.2589, 0.0977, 0.0521, and 0.0411 mW respectively. These results reveal that the sensor dissipated power when $R_L = R_{L,MAX}$ ($P_{S,RL,MAX}$) decreases with an increase in $R_{L,MAX}$ value. LPG, the base gas, has the highest value of $P_{S,RL,MAX}$ (0.3125 mW), this is because at $R_{L,MAX}$, the sensor current will be maximum and it decreases for the other gases because of the increase in the $R_{L,MAX}$. It can also be seen from the results that, the maximum value $P_{S,RL,MAX}$ (0.3125 mW) is far less than the tolerable value (15 mW [31]).

It can be seen from Figure 4, that the initial value of $R_{L,MAX}$ ($R_{L,MAX,i}$) which is maximum for each of the gases was obtained when $x = 200$ ppm. The value of $R_{L,MAX}$ decreases from $R_{L,MAX,i}$ to the final value ($R_{L,MAX,f}$) which is the minimum for each of the gases at $x = 10000$ ppm. It is also observed that the base gas has the minimum values of both $R_{L,MAX,i}$ and $R_{L,MAX,f}$ compared to other gases. $R_{L,MAX}$ generally, decreases with increasing x and its value at any concentration can be determined from Figure 4 for all MQ-6 gas sensor associated gases. The graph of Figure 4 revealed that $R_{L,MAX}$ depends on both the gas type and concentration.

As shown in Figure 5, the initial and final sensor circuit output voltages ($V_{RL,i}$ and $V_{RL,f}$) are attained when the values of x are 200 and 10,000 ppm respectively, for $R_L = 20$ k Ω . Also, the initial and final sensor circuit output voltages when $R_L = R_{L,MAX}$ ($V_{RL,MAX,i}$ and $V_{RL,MAX,f}$) are attained when the values of x are 200 and 10,000 ppm, respectively. The output voltage span when $R_L = 20$ k Ω and $R_L = R_{L,MAX}$ are denoted by $V_{RL,SP}$ and $V_{RL,MAX,SP}$ respectively. It can be seen in the Figure 5 that $V_{RL,MAX,i} > V_{RL,i}$ and $V_{RL,MAX,f} > V_{RL,f}$ except for LPG where $V_{RL,MAX,i} = V_{RL,i}$ and $V_{RL,MAX,f} = V_{RL,f}$ because $R_L = R_{L,MAX} = 20$ k Ω . For CH₄, H₂, Alcohol and CO $V_{RL,MAX,SP} > V_{R,LSP}$ while $V_{RL,MAX,SP} = V_{RL,SP}$ for LPG. It can be seen from Figure 5 that there is an improvement in both the span and range of sensor circuit output voltage when $R_L = R_{L,MAX}$ compared to when $R_L = 20$ k Ω . In summary, the study revealed that the sensitivity of the sensor circuit is maximum when $R_L = R_{L,MAX}$, $P_{S,RL,MAX} < 15$ mW (the maximum sensor power dissipation threshold [31]) and the sensor circuit output voltage span is maximum when $R_L = R_{L,MAX}$ for each of the gases. Based on these results the optimum value for R_L is $R_{L,MAX}$.

4. CONCLUSIONS

The technique for determining the MQ-series gas sensors circuit optimum R_L value for a given value of gas concentration was established. The method is appropriate for the determination of R_L when a gas sensor circuit with a very sensitive alarm point is to be designed. For a given value of R_O and x , the sensor circuit dynamics model equations were used for determining: (i) S as a function of R_L and (ii) P_S as a function of R_L . It was discovered that R_L must be tuned to R_O to obtain S_M for LPG which is the base gas and the value remains constant for any value of R_O . The $R_L = 20$ k Ω recommended for MQ-6 gas sensors in the datasheet when the LPG concentration is 1000 ppm was reinforced in this study, yielding S_M and tolerable P_S of 0.5143 mV/ppm and 0.3125 mW, respectively. The proposed method for the determination of R_L is time-saving, cost-effective, flexible and reliable.

Based on the dependence of both P_S and S on R_O as revealed in this study for LPG which is the base gas, it is recommended that the MQ-series sensor manufacturers devise a means of increasing the value of R_O so that lower P_S at S_M can be achieved. The findings will also aid the sensor circuit calibration process since the determined optimum R_L ($R_{L,MAX}$) will give S_M , acceptable P_S and an improvement in both the range and span of the sensor circuit output voltage. The study revealed that the R_L range in the datasheet (10 k $\Omega \leq R_L \leq 47$ k Ω) must be extended to (10 k $\Omega \leq R_L \leq 180$ k Ω) so that $R_{L,MAX}$ can be obtained for all the MQ-6 associated gases. The dependence of $R_{L,MAX}$ value on gas type and concentration is also parametrically revealed in the study. Finally, the optimal results can be obtained from the MQ-series gas sensor circuit when the condition $R_L = R_{L,MAX}$ is met for a given gas type and concentration.




REFERENCES

- [1] A. Popa *et al.*, "An intelligent IoT-based food quality monitoring approach using low-cost sensors," *Symmetry*, vol. 11, no. 3, pp. 374, Mar. 2019, doi: 10.3390/sym11030374.
- [2] H. Baha and Z. Dibi, "A novel neural network-based technique for smart gas sensors operating in a dynamic environment," *Sensors*, vol. 9, no. 11, pp. 8944-8960, Nov. 2009, doi: 10.3390/s91108944.
- [3] A. A. Taiwo, O. J. Femi, A. O. Yusuf, and P. J. Olusogo, "Analytical determination of load resistance value for MQ-series gas sensors: MQ-6 as case study," *TELKOMNIKA Telecommunication, Computing, Electronics and Control*, vol. 19, no. 2, pp. 575-582, Apr. 2021, doi: 10.12928/TELKOMNIKA.v19i2.17427.
- [4] R. Rumantri, M. Y. N. Khakim, and I. Iskandar, "Design and characterization of low-cost sensors for air quality monitoring system," *Jurnal Pendidikan IPA Indonesia*, vol. 7, no. 3, pp. 347-354, Sept. 2018, doi: 10.15294/jpii.v7i3.14444.
- [5] V. Deotalu, A. Loyare, C. Dandekar, and R. Mandi, "Real Time Olfaction Monitoring system & Implementation of E-sensing Technique in Electronic Nose," *International Research Journal of Engineering and Technology*, vol. 4, no. 4, pp. 858-863, 2017. [Online]. Available: <https://www.irjet.net/archives/V4/i4/IRJET-V4I4175.pdf>
- [6] K. V. D. Ambeth, "Human security from death defying gases using an intelligent sensor system," *Sensing and bio-sensing research*, vol. 7, pp. 107-114, Mar. 2016, doi: 10.1016/j.sbsr.2016.01.006.
- [7] Q. Ding, D. Zhao, J. Liu, and Z. Yang, "Detection of fruits in warehouse using Electronic nose," in *MATEC Web of Conferences*, vol. 232, p. 04035, Jan. 2018, doi: 10.1051/mateconf/201823204035.
- [8] J. Y. Kim, S. W. Kang, T. Z. Shin, M. K. Yang, and K. S. Lee, "Design of a smart gas sensor system for room air-cleaner of automobile-thick-film metal oxide semiconductor gas sensor," in *International Forum on Strategic Technology*, pp. 72-75, 2006, doi: 10.1109/IFOST.2006.312250.
- [9] A. Kanade and A. Shaligram, "Development of an E-Nose using metal oxide semiconductor sensors for the classification of climacteric fruits," *International Journal of Scientific & Engineering Research*, vol. 5, no. 2, Feb. 2014, doi: 10.14299/ijser.2014.02.003.
- [10] J. Chilo, J. Pelegri-Sebastia, M. Cupane, and T. Sogorb, "E-nose application to food industry production," *IEEE Instrumentation & Measurement Magazine*, vol. 19, no. 1, pp. 27-33, 2016, doi: 10.1109/MIM.2016.7384957.
- [11] K. Vandana, C. Baweja, D. Simmarpreet, and S. Chopra, "Influence of Temperature and Humidity on the Output Resistance Ratio of the MQ-135 Sensor," *Int. J. Adv. Res. Comput. Sci. Softw. Eng.*, vol. 6, no. 4, pp. 423-429, 2016. [Online]. Available: <https://www.researchgate.net/deref/http%3A%2F%2Fwww.ijarcsse.com%2F>.
- [12] H. Baha and Z. Dibi, "Ann modeling of a gas sensor," *Journal of Electrical Engineering and Technology*, vol. 5, no. 3, pp. 493-496, 2010, doi: 10.5370/JEET.2010.5.3.493.
- [13] K. Lamamra and D. Rechem, "Artificial neural network modelling of a gas sensor for liquefied petroleum gas detection," in *8th International Conference on Modelling, Identification and Control (ICMIC)*, pp. 163-168, 2016, doi: 10.1109/ICMIC.2016.7804292.
- [14] M. Fezari, R. Hattab, and A. Al-Dahoud, "Oak Ridge Air Quality Index Computation: a way for Monitoring Pollutions in Annaba City," in *International Arab Conference on Information Technology (ACIT)*, 2015. [Online]. Available: https://www.researchgate.net/publication/290429944_Oak_Ridge_Air_Quality_Index_Computation_a_way_for_Monitoring_Pollutions_in_Annaba_City.
- [15] S. Kouda, A. Dendouga, S. Barra, and T. Bendib, "Design of a selective smart gas sensor based on ANN-FL hybrid modeling," *Journal of Nano- and Electronic Physics*, vol. 10, no. 6, Dec. 2018, doi: 10.21272/jnep.10(6).06011.
- [16] Z. Nenova and G. Dimchev, "Compensation of the impact of disturbing factors on gas sensor characteristics," *Acta Polytech. Hung.*, vol. 10, no. 3, pp. 97-111, 2013, [Online]. Available: http://acta.uni-obuda.hu/Nenova_Dimchev_41.pdf
- [17] M. Rakesh and A. A. Prabakar, "Gas Sensor profiling," presented at the *Proceedings of Annual Seminar on C-DAC Noida Technologies (ASCNT)*, pp. 1-5, 2011, [Online]. Available: https://www.academia.edu/23893651/Response_Profiling_of_gas_sensors_2011_Final.
- [18] A. Shahid, J. H. Choi, A. H. S. Rana, and H. S. Kim, "Least squares neural network-based wireless E-Nose system using an SnO₂ sensor array," *Sensors*, vol. 18, no. 5, p. 1446, May 2018, doi: 10.3390/s18051446.
- [19] Q. A. Al-Haija, H. Al-Qadeeb, and A. Al-Lwaimi, "Case Study: Monitoring of AIR quality in King Faisal University using a microcontroller and WSN," *Procedia Computer Science*, vol. 21, pp. 517-521, 2013, doi:10.1016/j.procs.2013.09.072.
- [20] B. B. L. Heyasa and R. G. V. R. Kristopher, "Initial Development and Testing of Microcontroller-MQ2 Gas Sensor for University Air Quality Monitoring," *IOSR Journal of Electrical and Electronics Engineering (IOSR-JEEE)*, vol. 12, no. 3, pp. 47-53, 2017, doi: 10.9790/1676-1203024753.
- [21] A. Biswal, J. Subhashini, and A. K. Pasayat, "Air quality monitoring system for indoor environments using IoT," in *AIP Conference Proceedings*, vol. 2112, no. 1, p. 020180, Jun. 2019, doi: 10.1063/1.5112365.
- [22] H. A. H. Nograles, C. P. D. Agbay, I. S. L. Flores, A. L. Manuel, and J. B. C. Salonga, "Low cost Internet-based wireless sensor network for air pollution monitoring using Zigbee module," in *2014 Fourth International Conference on Digital Information and Communication Technology and its Applications (DICTAP)*, pp. 310-314, 2014, doi: 10.1109/DICTAP.2014.6821702.
- [23] S. N. Mahmood, A. J. Ishak, and S. T. Hussain, "GSM based gas leak monitoring system," *Periodicals of Engineering and Natural Sciences*, vol. 7, no. 2, pp. 670-678, Aug. 2019, doi: 10.21533/pen.v7i2.529.
- [24] S. Natarajan, P. Deshpande, P. Gole, and P. Bhosale, "LPG Gas Detector and Prevention," *International Journal of Current Research*, vol. 9, pp. 60140-60142, 2017, [Online]. Available: <https://www.journalcra.com/sites/default/files/issue-pdf/26923.pdf>
- [25] M. W. Siddiqui and H. K. Mishra, "LPG Leakage Detection and Prevention," *Imperial Journal of Interdisciplinary Research (IJIR)*, vol. 3, pp. 1084-1086, May, 2017, Corpus ID: 117160604.
- [26] Z. Chafekar, M. H. Khan, K. Lakra, and S. Dhonde, "Implementation of automatic gas accident prevention system using Arduino and gsm," *International Journal of Computer Applications*, vol. 180, no. 47, pp. 5-7, 2018. [Online]. Available: <https://www.ijcaonline.org/archives/volume180/number47/chafekar-2018-ijca-917242.pdf>
- [27] K. B. Suarsana, A. A. N. Gunawan, and N. N. Ratini, "LPG Leakage Control Using SMS through SIM800L with MQ-2 Sensor and Stepper Motor Based on Arduino UNO," *Advances in Applied Physics*, vol. 6, no. 1, pp. 15-18, 2018, doi: 10.12988/aap.2018.814.
- [28] T. Ismail, D. Das, J. Saikia, J. Deka, and R. Sarma, "GSM based gas leakage warning system," *International Journal of Advanced Research in Computer and Communication Engineering*, vol. 3, no. 4, pp. 2278-1021, Apr. 2014. [Online]. Available: https://www.academia.edu/download/45847510/IJARCCCE4C__a__Jyotirmoy__GSM_Based_Gas_Leakage.pdf




- [29] A. Suyuti, A. Ahmad, and A. E. U. Salam, "Intelligent system of LPG gas leakage detection for web-based living house security," ICIC express letters. Part B, Applications: an international journal of research and surveys, vol. 10, no. 2, pp. 89-96, 2019, doi:10.24507/icicelb.10.02.89.
- [30] A. A. Meenakshi, R. B. N. Meghana, and P. R. Krishna, "LPG Gas Leakage Detection and Prevention System," International Journal on Future Revolution in Computer Science & Communication Engineering (IJFRCSCCE), vol. 3, pp. 1-4, 2017. [Online]. Available: <http://www.ijfrcsce.org/index.php/ijfrcsce/article/view/169>.
- [31] S. M. Hadi, W. R. Abdulmajeed, and M. M. Thib, "Design and Implement a Gas Pipeline Inspection System using Robotic Vehicle," Journal of Information Engineering and Applications, vol. 4, no. 9, pp. 49-56, 2014. [Online]. Available: <https://iiste.org/Journals/index.php/JIEA/article/view/15508>.
- [32] Hanwei Technical Data MQ-6 Gas Sensor, [Online]. Available: <https://www.sparkfun.com/datasheets/Sensors/Biometric/MQ-6.pdf>

BIOGRAPHIES OF AUTHORS






Dr. Ajiboye Aye Taiwo    is a Council for Regulation of Engineering in Nigeria (COREN) Registered Engineer and a Member of the Nigerian Society of Engineers (NSE). Obtained a Bachelor of Science degree in Electrical Engineering from the University of Ibadan, Ibadan, Nigeria in 1989. He obtained a Master of Engineering degree and a Doctoral degree in Electrical Engineering from University of Ilorin, Ilorin, Nigeria in 2005 and 2012 respectively. He is a senior lecturer in the Department of Computer Engineering, University of Ilorin, Ilorin, Nigeria and his research interests have been in Instrumentation and Control Systems design, simulation, and development. He can be contacted at email: ajiboye.at@unilorin.edu.ng.






Dr. Opadiji Jayeola Femi    is a Reader in the Department of Computer Engineering, University of Ilorin, Ilorin, Nigeria with over twenty years work experience in the academia and the engineering industry. He obtained his Bachelor of Engineering (B.Eng.) and Master of Engineering (M.Eng.) degrees in Electrical Engineering from the University of Ilorin, Nigeria and a Doctor of Engineering (Dr.Eng.) degree in Computer and System Engineering from Kobe University, Japan. Dr. Opadiji is a Council for Regulation of Engineering in Nigeria (COREN) Registered Engineer and a Member of the Nigerian Society of Engineers (NSE). His area of specialization is System Informatics and his research interests cut across optimization of complex systems, multiagent systems, industry 4.0 and science and engineering education. He can be contacted at email: jopadiji@unilorin.edu.ng.



Ajayi Adebimpe Ruth    holds a B. Tech degree in Computer Engineering from, Ladoke Akintola University of Technology (LAUTECH), Ogbomosho, Oyo State, Nigeria in 2008 and M.Eng. degree in Electrical and Electronics Engineering from the University of Ilorin, Ilorin, Kwara State, Nigeria in 2021. She is currently a Lecturer II in the department of Computer Engineering of the same University. Her current research interest include: digital signal processing and machine learning. She can be contacted at email: ajayi.ra@unilorin.edu.ng.



Popoola Joshua Olusogo    is a Research Fellow in the Department of Computer Engineering, University of Ilorin, Ilorin, Nigeria. He obtained his Bachelor of Engineering (B.Eng.) degree in Electrical Engineering from the University of Ilorin, Nigeria in 1995 and Master of Science (M.Sc.) degree in Computer and Network Engineering from Sheffield Hallam University, United Kingdom in 2017. He is a Council for Regulation of Engineering in Nigeria (COREN) Registered Engineer and a Member of the Nigerian Society of Engineers (NSE). He can be contacted at email: olusogo@unilorin.edu.ng.